JAERI-M
92-195

VERIFICATION OF COMPUTER CODE FPRETAIN WITH RESPECT TO RIA DATA FROM SPERT AND PBF EXPERIMENTS

December 1992

Young-ho HEO* and Kazuaki YANAGISAWA

日本原子力研究所
Japan Atomic Energy Research Institute

JAERI-Mレポートは，日本原子力研究所が不定期に公刊している研究報告書です。
入手の問合わせは，日本原子力研究所技術情報部情報資料課（〒319-11茨城県那珂郡東海村）あて，お申しこしください。なお，このほかに財団法人原子力弘済会資料センター（〒319-11 茨城県那珂郡東海村日本原子力研究所内）で複写による実費頒布をおこなっております。

JAERI-M reports are issued irregularly.
Inquiries about availability of the reports should be addressed to Information Division Department of Technical Information, Japan Atomic Energy Research Institute, Tokai-mura, Naka-gun, Ibaraki-ken 319-11, Japan.

編集兼発行　日本原子力研究所
印　　刷　いばらき印刷㈱

JAERI-M 92-195

Verification of Computer Code FPRETAIN with respect to RIA Data from SPERT and PBF Experiments

Young-ho HEO* and Kazuaki YANAGISAWA

Department of Fuel Safety Research
Tokai Research Establishment
Japan Atomic Energy Research Institute
Tokai-mura, Naka-gun, Ibaraki-ken

(Received November 24, 1992)

This report presents the comparisons between calculated and measured fuel rod behavior and the analysis of stress for preirradiated LWR type fuel rods during reactivity initiated accident (RIA) conditions. For the calculations, FPRETAIN computer code which can simulate the fuel behavior under RIA conditions at extended burnup stage was used. For the experimental, data obtained from the Special Power Excursion Reactor Test (SPERT) and the Power Burst Facility (PBF) tests were used. The results of the comparisons showed that the FPRETAIN code predicted well the tendency of the fuel rod behavior during RIA. From the results of the stress analysis, it was found that the maximum hoop stress of cladding was not proportional to the energy deposition of fuel rod. Calculated cladding maximum hoop stress of failed fuel at high burnup was not lower than that of intact fresh or low burnup fuel.

Keywords: Fuel Behavior, RIA, Preirradiated, Computer Code, FPRETAIN, Hoop Stress

---

* Korea Atomic Energy Research Institute

米国ＳＰＥＲＴ及びＰＢＦの反応度事故実験データを用いた計算コードＦＰＲＥＴＡＩＮの検証

日本原子力研究所東海研究所燃料安全工学部
許　英豪* ・柳澤　和章

（1992年11月24日受理）

本報は，反応度事故（ＲＩＡ）条件下における予備照射済軽水炉型燃料棒について計算値及び実測値による比較並びに応力解析の結果を行ったものである。計算には，ＲＩＡ条件における高燃焼度燃料棒ふるまいを模擬できる計算コードＦＰＲＥＴＡＩＮを使用した。実験には，Special Power Excursion Reactor Test（ＳＰＥＲＴ）及びPower Burst Facility（ＰＢＦ）からのデータを使用した。比較結果によれば，ＦＰＲＥＴＡＩＮはＲＩＡ時の燃料のふるまいをよく予測する傾向にあった。応力解析の結果によれば，燃料被覆管の最大円周応力は燃料に付加された発熱量に比例して増加しないことが分かった。高燃焼度領域で破損した燃料棒に生じた被覆最大円周応力計算値は，非破損であった未照射燃料棒や低燃焼度燃料棒のそれらと比較して，低くなかった。

東海研究所：〒319－11　茨城県那珂郡東海村白方字白根２－４
＊韓国原子力研究所

Contents

目　　次

1. Introduction

The reactivity initiated accident (RIA) has long been recognized as one of the important safety considerations. The rapid inadvertent insertion of reactivity into a light water reactor core can lead to high cladding temperatures and to cause fuel rod failure. Since fuel rod failure can lead to reactor destruction, safety concerns about the RIA have been highlighted on the fuel rod failure behavior.

To understand the behavior of fuel rods under RIA, a number of experiments have been performed and progressing in the world. Much of the experimental data on fuel rod behaviour during the RIA were obtained from Special Power Excursion Reactor Test (SPERT)[1] and from Power Burst Facility (PBF)[2], and more recently from Nuclear Safety Research Reactor (NSRR)[3] test programs.

The mode of fuel rod failure during RIA seems to be strongly affected by previous irradiation and peak fuel enthalpy. The modes of unirradiated fuel rod failure can be grouped into some categories[4], hence (a) fracturing and embrittlement failure of the cladding as a result of extensive oxidation at the cladding outer surface due to film boiling and (b) ballooning of cladding for the case of pressurized test fuel. At higher energy deposition, it is possible to occur fuel failure (c) due to cladding melt or breach by heat transfer from either solid or molten UO_2 fuel in contact with the cladding. For preirradiated fuels, pellet-cladding mechanical interaction (PCMI) at the cladding inner surface is also a possible cause of fuel failure.

According to the experimental results[2,5], it is known that the failure threshold energy of preirradiated fuel rod tends to decrease from that of unirradiated fuel rod. The cause of failure in preirradiated fuel is considered to be PCMI. To understand PCMI during RIA, stress or strain calculations by computer code is effective.

The main purpose of this report is to study the stress state related to the fuel rod failure caused by PCMI during RIA, by using the computer code calculations taking into accounts experimental results. In doing so, the calculations were conducted with FPRETAIN computer code which has been developed to simulate the fuel behavior under RIA at extended burnup stage. The outline of the code is described elsewhere[6,7]. The code consists of thermal and mechanical parts as shown in the flow chart of Figure 1. The result of calculation is compared with that of experiment performed in PBF and in SPERT/CDC.

2. Description of Experiments

In this section, RIA test data prepared for calculation are described. All data used here were from open literatures[8-12].

The fuel rod characteristics, pre-irradiation conditions, and RIA test conditions of the PBF experiments are summarized in Table 1. The scoping tests[8] consisted of four separate single rod tests with unirradiated LWR type fuel rods. While, RIA-ST-4 fuel rod used in the PBF scoping test was not used in this study because of very high energy deposition (695 cal/g-UO_2 radial average total energy deposition). The four unirradiated test fuel rods were subjected to one or more power transients resulting in total radial average energy depositions ranging from 250 to 345 cal/g-UO_2 (185 to 260 cal/g-UO_2 maximum axial peak radial average fuel enthalpies). The test RIA 1-1[9] was conducted with four separately shrouded LWR type fuel rods, where two were unirradiated and two were preirradiated. The rods were subjected to a single power transient resulting in a radial average total energy deposition of 365 cal/g-UO_2 (285 cal/g-UO_2 axial peak radial average fuel enthalpy). The test RIA 1-2[10] was performed with four separately shrouded LWR type fuel rods, with preirradiated fuels. The rods were subjected to a single power transient resulting in a radial average total energy deposition of 240 cal/g-UO_2 (185 cal/g-UO_2 axial peak radial average fuel enthalpy). In all cases, the coolant conditions during the transients were similar to a BWR-6 assembly at zero power hot startup conditions (538 °K, 6.45 MPa and 85 cm^3/s, coolant temperature, pressure and flow rate, respectively).

Regarding SPERT/CDC, the fuel rod design, preirradiation conditions, and RIA test conditions are summarized in Table 2. Ten tests[11,12] were used in the CDC where two GEP (General Electric Prototype) rods had burnups of about 1000 MWd/MtU and eight GEX (General Electric Experimental) rods had burnups in the range of 3000 to 32000 MWd/MtU. The total energy depositions of fuel rods during the transients ranged from 161 to 348 cal/g-UO_2. In all cases, the coolant conditions during the transients were similar to BWR cold startup condition (ambient temperature and pressure, with zero flow rate).

3. Result of Calculation

Energy depositions and linear powers of the PBF test RIA 1-2 and of the SPERT/CDC test RIA (Test No. 685) at the axial peak power location during RIA, used for the FPRETAIN calculation, are shown in Figures 2 and 3, respectively.

Calculated pellet and cladding temperatures at the axial peak power location versus energy deposition at the PBF test 1-2 (Rod No. 802-2) and the SPERT/CDC test (Test No. 685) are shown in Figures 4 and 5, respectively. As shown, pellet center and surface temperatures increase with increasing energy deposition. While cladding inside and outside temperatures quickly increase near the total energy depositions. The maximum pellet centerline temperatures of the PBF rod (802-2) and the SPERT/CDC rod (685) reach to the amounts of 2090°C at 240 cal/g-UO_2 and 1780°C at 186 cal/g-UO_2, respectively. Maximum cladding surface temperatures of the PBF rod (802-2) and SPERT/CDC rod (685) are 1500°C at 240 cal/g-UO_2 and 1225°C at 186 cal/g-UO_2, respectively.

In Figures 6 and 7, calculated fission gas releases (FGR) at the axial peak power location for PBF test RIA 1-2 (Rod No. 802-2) and for SPERT/CDC test RIA (Test No. 685) are shown, respectively. FGR increased rapidly up to energy deposition of 100 cal/g-UO_2 and remained almost constant after that. The maximum FGR of PBF rod (802-2) and that of SPERT/CDC rod (685) are about 11% and 30%, respectively.

In Figures 8 and 9, pellet and cladding diametral displacements at the axial peak power location in PBF test RIA 1-2 (Rod No. 802-2) and in SPERT/CDC test RIA (Test No. 685) are shown, respectively. Deformation at mid-pellet location is greater than that at pellet-to-pellet interface one. The cladding maximum diametral displacements of the PBF rod (802-2) and the SPERT/CDC rod (685) at mid-pellet are 96 μm at 240 cal/g-UO_2 and 61 μm at 186 cal/g-UO_2, respectively.

In Figures 10 and 11, cladding maximum hoop stresses at each time step and the average diametral gaps in PBF test RIA 1-2 (Rod No. 802-2) and in SPERT/CDC test RIA (Test No. 685) are shown, respectively. After gap closure, cladding hoop stress increased quickly and then relaxed. The maximum hoop stresses of the PBF rod (802-2) and the SPERT/CDC rod (685) are 372 MPa at 205 cal/g-UO_2 and 550 MPa at 176 cal/g-UO_2, respectively.

4. Comparison with Experiment

Figures 12 and 13 show the comparison between the thermo-couple measured[13] and calculated cladding surface temperatures at the 0.79 m bottom of fuel location on the PBF test RIA 1-2 fuel rods (Rod No. 802-1 and 802-2). Calculated cladding peak temperatures are higher than the measured. Peak temperatures determined from the oxide thickness measurements[14] were relatively close to the calculated peak temperatures in both cases.

Figure 14 shows the comparison between calculated and measured rod internal pressure[13] from the PBF test RIA 1-2 fuel rod (Rod No. 802-2). Calculated rod internal pressure is in good agreement with measurement.

Comparisons between measured[11,13] and calculated cladding elongation for the PBF test RIA (Rod No. 802-2) and the SPERT/CDC test RIA (Test No. 685) are shown in Figures 15 and 16, respectively. In both cases, the calculated values are lower than the measured.

Experiments[10,11] showed that the SPERT/CDC test RIA fuel rod (Test No. 859) and the PBF test RIA 1-2 fuel rod (Rod No. 802-3) failed in the early stage of transient. The SPERT/CDC rod (Test No. 859) failed during transient when energy deposition reached 85 cal/g-UO_2. While PBF RIA 1-2 rod (Rod No. 802-3) failed with 22 small longitudinal cracks at the fuel rod locations between ~18 cm and ~72 cm from the bottom of the fuel stack. The radial average peak fuel enthalpy at the 18 cm and 72 cm locations was about 140 cal/g-UO_2 (about 182 cal/g-UO_2 in the radial average energy deposition). It is considered that the fracture or tearing of preir-radiated cladding was caused by pellet-cladding mechanical interaction (PCMI) resulting from high-strain-rate deformation of the relatively cool alpha-phase Zircaloy[2].

In Figure 17, the FPRETAIN calculated cladding maximum hoop stresses of the PBF tests and the SPERT/CDC tests are plotted against burnup. In case of the SPERT/CDC rod (Test No. 859), cladding maximum hoop stress was about 520 MPa, while that of PBF rod (Rod No. 802-3) was about 416 MPa. The calculated hoop stress for fuel failure did not change significantly with increase of burnup.

In Figure 18, cladding maximum hoop stress of PBF and SPERT/CDC is shown as a function of total energy deposition. Cladding maximum hoop stresses did not change significantly with increase of total energy deposition.

5. Concluding Remarks

Concluding remarks obtained from the present study are:

(1) The calculated cladding surface temperatures were higher than the measured. However, when one takes the measured oxide layer thickness at the thermo-couple locations into consideration, calculated temperatures were relatively close to measured.

(2) The calculated rod internal pressure is relatively agreed well with the measurement.

(3) Calculated cladding maximum hoop stress of preirradiated fuel up to burnup of 32000 MWd/MtU did not change significantly.

Acknowledgment

The authors would like to thank the colleagues of Reactivity Accident Laboratory and in particular Dr. T. Fujishiro, Head of Reactivity Accident Laboratory, for his valuable comments and encouragement in the preparation of this report. The authors also wish to thank Mr. H. Saito and Mr. M. Kato of CRC Research Institute, Inc. for their assistance to the calculation of the computer code.

5. Concluding Remarks

Concluding remarks obtained from the present study are:

(1) The calculated cladding surface temperatures were higher than the measured. However, when one takes the measured oxide layer thickness at the thermo-couple locations into consideration, calculated temperatures were relatively close to measured.

(2) The calculated rod internal pressure is relatively agreed well with the measurement.

(3) Calculated cladding maximum hoop stress of preirradiated fuel up to burnup of 32000 MWd/MtU did not change significantly.

Acknowledgment

The authors would like to thank the colleagues of Reactivity Accident Laboratory and in particular Dr. T. Fujishiro, Head of Reactivity Accident Laboratory, for his valuable comments and encouragement in the preparation of this report. The authors also wish to thank Mr. H. Saito and Mr. M. Kato of CRC Research Institute, Inc. for their assistance to the calculation of the computer code.

References

(1) T. Fujishiro et al., "Light Water Reactor Fuel Response during Reactivity Initiated Accident Experiments", NUREG/CR-0269, 1978.

(2) P.E. MacDonald et al., "Assessment of Light Water Reactor Fuel Damage during a Reactivity Initiated Accident", Nuclear Safety, Vol. 21, No.5, p582-602, 1980.

(3) M. Ishikawa et al., "A Study of Fuel Behavior under Reactivity Initiated Accident Conditions-Review", Journal of Nuclear Materials, Vol. 95, p1-30, 1980.

(4) T. Fujishiro et al., "Fuel Behavior during Simulated Reactivity Initiated Accidents in the NSRR Experiments and Its Application", Proc. Annual CNA/CNS Conf. Canada, July, 1987.

(5) T. Fujishiro et al., "Transient Fuel Behavior of Preirradiated PWR Fuels under Reactivity Initiated Accident Conditions", Journal of Nuclear Materials, Vol. 188, p162-167, 1992.

(6) K. Yanagisawa, "Development and Verification of the FP Behavior Evaluation Computer Code: FPRETAIN - Release and Retention of FP from Pre-Irradiated Fuel Rods", JAERI-M 89-095, 1989 (in Japanese).

(7) K. Yanagisawa et al., "Simulations by Computer Codes FEMAXI-III and FPRETAIN for In-core Behavior of LWR Fuel", First International Conference on Supercomputing in Nuclear Applications, March 12-16, Japan, 1990.

(8) R.S. Semken et al., "Reactivity Initiated Accident Test Series, RIA Scoping Tests Fuel Behavior Report", NUREG/CR-1306, EGG-2024, April 1980.

(9) S.L. Seiffert et al., "Reactivity Initiated Accident Test Series, Test RIA 1-1 Fuel Behavior Report", NUREG/CR-1465, EGG-2040, September 1980.

(10) B.A. Cook et al., "Reactivity Initiated Accident Test Series, Test RIA 1-2 Fuel Behavior Report", NUREG/CR-1842, EGG-2073, January 1981.

(11) R.W. Miller, "The Effects of Burnup on Fuel Failure-Power Burst Tests on Fuel Rods with 13,000 and 32,000 MWd/MtU Burnup", ANCR-1280, January 1976.

(12) R.W. Miller, "The Effects of Burnup on Fuel Failure-Power Burst Tests on Low Burnup UO_2 Fuel Rods", IN-ITR-113, July 1970.

(13) C.L. Zimmermann et al., "Experimental Data Report for Test RIA 1-2 (Reactivity Initiated Accident Test Series)", NUREG/CR-0765, Tree-

1271, June 1979.

(14) S.K. Fukuda et al., "A Comparison of Measured and Calculated LWR Fuel Behavior during a Hypothetical Reactivity Initiated Accident", CONF-800723--7.

Table 1 PBF test RIA summary

Item \ Test No.	RIA-ST[1]				RIA 1-1				RIA 1-2			
	ST1 (PB1)	ST1 (PB2)	ST-2	ST-3	801-3	801-5	801-1	801-2	802-1	802-2	802-3	802-4
Fuel Rod Design[2]												
fuel form	dished UO_2 pellet											
enrichment (%)	5.8								5.7			
pellet dia. (mm)	8.23				8.53				8.59			
pellet length (mm)	15.24											
stack length (mm)	914.4											
pellet density (%TD)	94.5								94.0			
cladding material	Zircaloy-4 (stress relieved, 50% cold worked)											
cladding O.D. (mm)	9.7				9.93		9.995		9.99			
cladding I.D. (mm)	8.42				8.75							
plenum vol. (cm³)	3.18		2.43		4.65							
gas pressure (MPa)	0.19				0.103							
gas composition	He, 100%				Air, 100%							
Pre-irradiation Condition												
reactor	no pre-irradiation				SAXTON, COREIII							
coolant					inlet temperature : 522°K							
					system pressure : 15.5MPa							
rod avg. burn up (MWD/MTU)					4600	4650	5220	5110	4430	4530		
rod power (kW/m)[3]							～ 9.2					
RIA Test Condition												
reactor	Power Burst Facility (PBF)											
test mode	single rod				four individually shrouded fuel rods							
start up condition	BWR hot start up (temp : 538°K, press : 6.45MPa, 0.085 L/S per rod)											
filling gas composition and pressure for test							77.7%He 22.3%Ar 0.1MPa	not opened	77.7%He 22.3%Ar 0.1MPa	not opened	2.43MPa	77.7%He 22.3%Ar 2.35MPa
total energy[4] (cal/g·UO_2)	250	330	345	300	365				240			
RIA Test Result												
rod failure	NO	YES	YES	NO	YES	YES	YES	YES	NO	NO	YES	NO

1) PBF RIA Scoping Test.

2) Data are nominal value before pre-irradiation.

3) Time-averaged linear power of Rod (802-4) at the axial peak location.

4) Radial avevage total energy depostion.

Table 2 SPERT/CDC test RIA summary

Item \ Test No.	GEX[1]								GEP[2]	
	571	568	567	569	684	685	756	859	703	709
Fuel Rod Design[3]										
fuel form	dished UO_2 pellet									
enrichment (%)	7.0									
pellet diameter (mm)	6.817								12.294	
pellet length (mm)	12.0								22.0	
stack length (mm)	132.0									
pellet density (%TD)	94.0									
cladding material	Zircaloy-2 (stress relieved, 10% cold worked)									
cladding O.D. (mm)	7.938								14.288	
cladding I.D. (mm)	6.922								12.662	
plenum vol. (cm^3)	0.5								1.6	
gas pressure (MPa)	0.103									
gas composition	He, 100%									
Pre-irradiation Condition										
reactor	Engineering Test Reactor (ETR)									
coolant	inlet temperature : 511°k, system pressure : 6.9MPa									
rod average burn up (MWD/MTU)	4550	3480	3100	4140	12900	13100	32700	31800	1140	990
rod power (kW/m)[4]	67.9	51.8	46.3	61.7	41.0	41.3	46.9	45.6	55.1	47.2
RIA Test Condition										
reactor	Capsule Driver Core (CDC)									
test mode	single rod									
start up condition	BWR cold start up (atmospheric pressure, ambient temperature and no forced coolant flow)									
total energy[5] (cal/g·UO_2)	161	199	264	348	200	186	176	190	192	238
RIA Test Result										
rod failure	NO	YES	YES	YES	NO	NO	YES	YES	NO	YES

1) General Electric Experimental.

2) General Electric Production or Proto type.

3) Data are nominal value before pre-irradiation.

4) Rod average linear power at maximum ETR power.

5) Radial average total energy deposition.

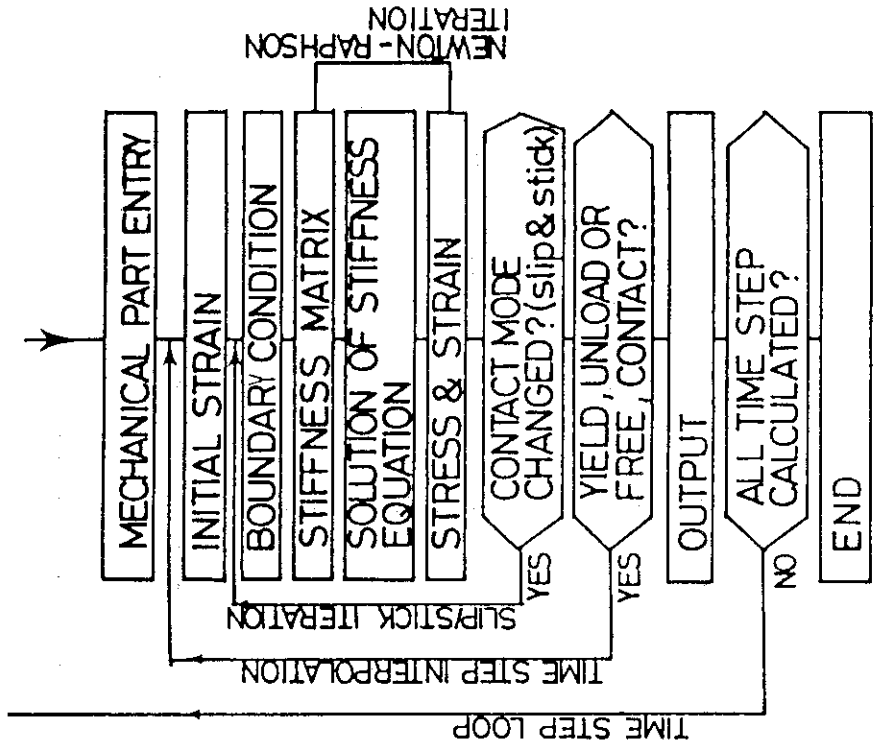

Fig. 1 Flow chart of FPRETAIN computer code.

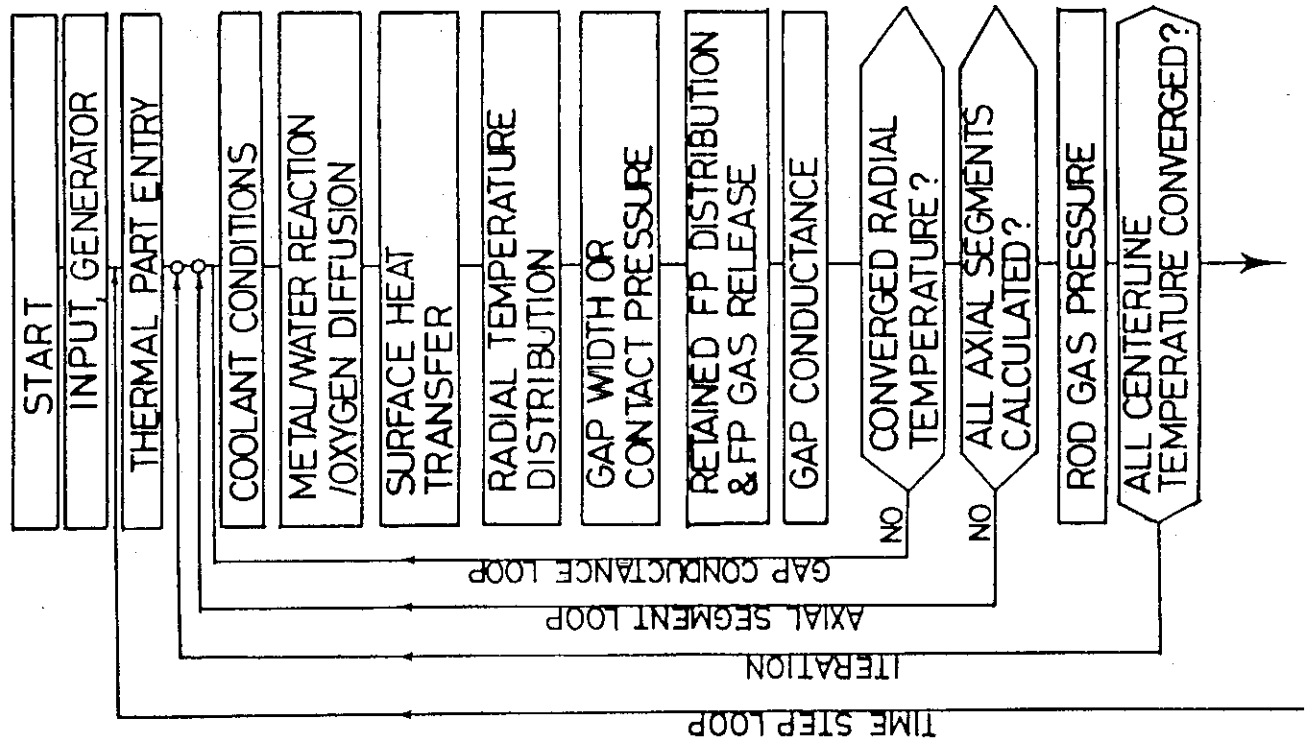

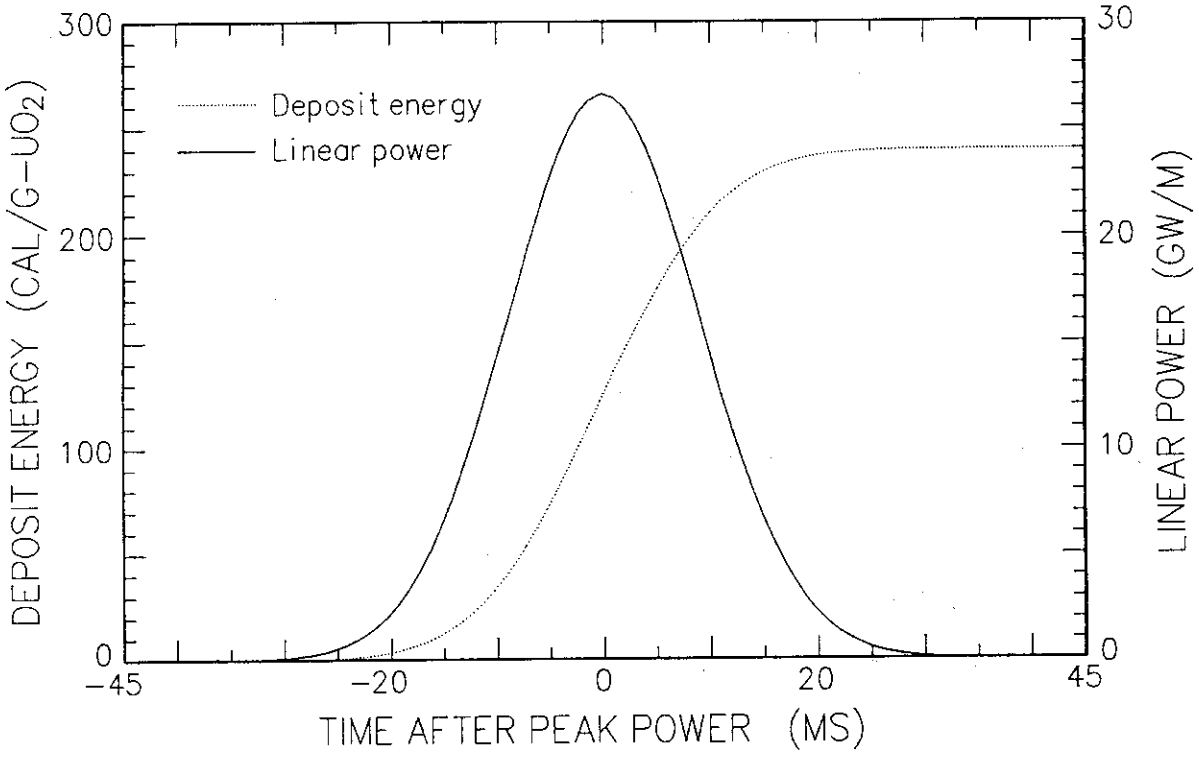

Fig. 2 Calculated deposit energy and linear power at the axial peak power location during the PBF test RIA 1-2 (Rod No. 802-2).

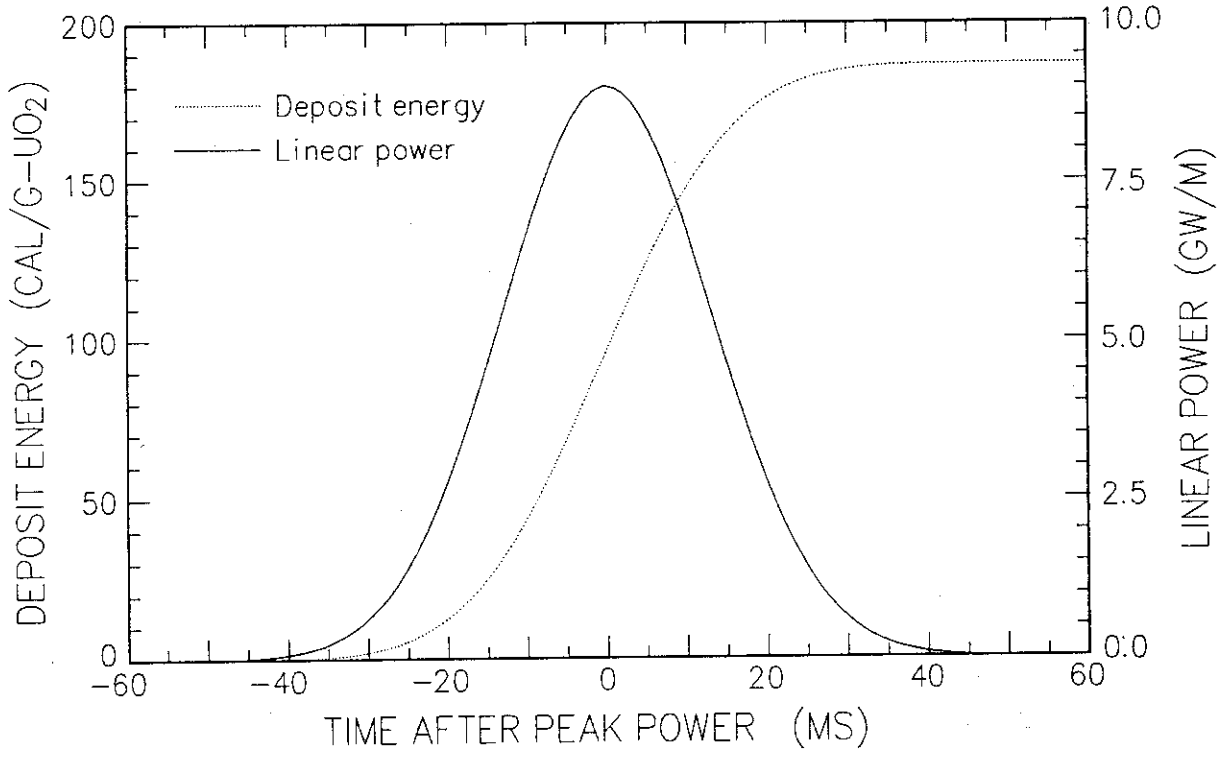

Fig. 3 Calculated deposit energy and linear power at the axial peak power location during the SPERT/CDC test RIA (Test No. 685).

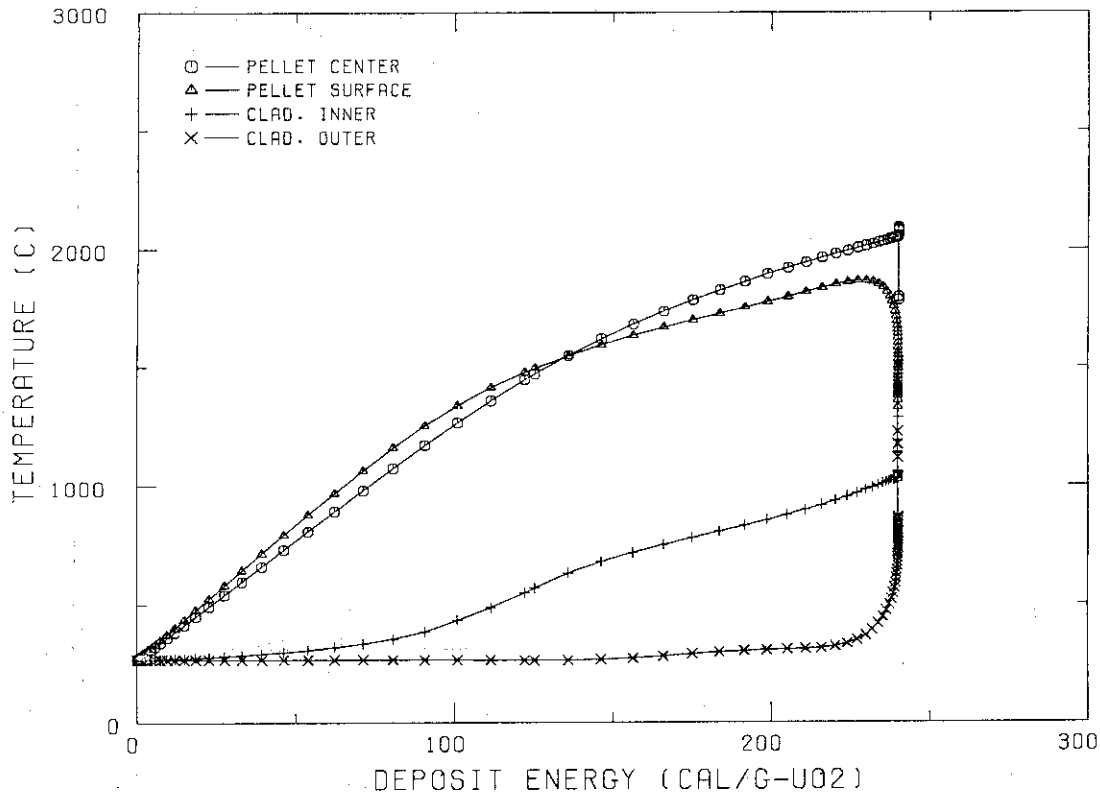

Fig. 4 Calculated pellet and cladding temperatures at the axial peak power location during the PBF test RIA 1-2 (Rod No. 802-2).

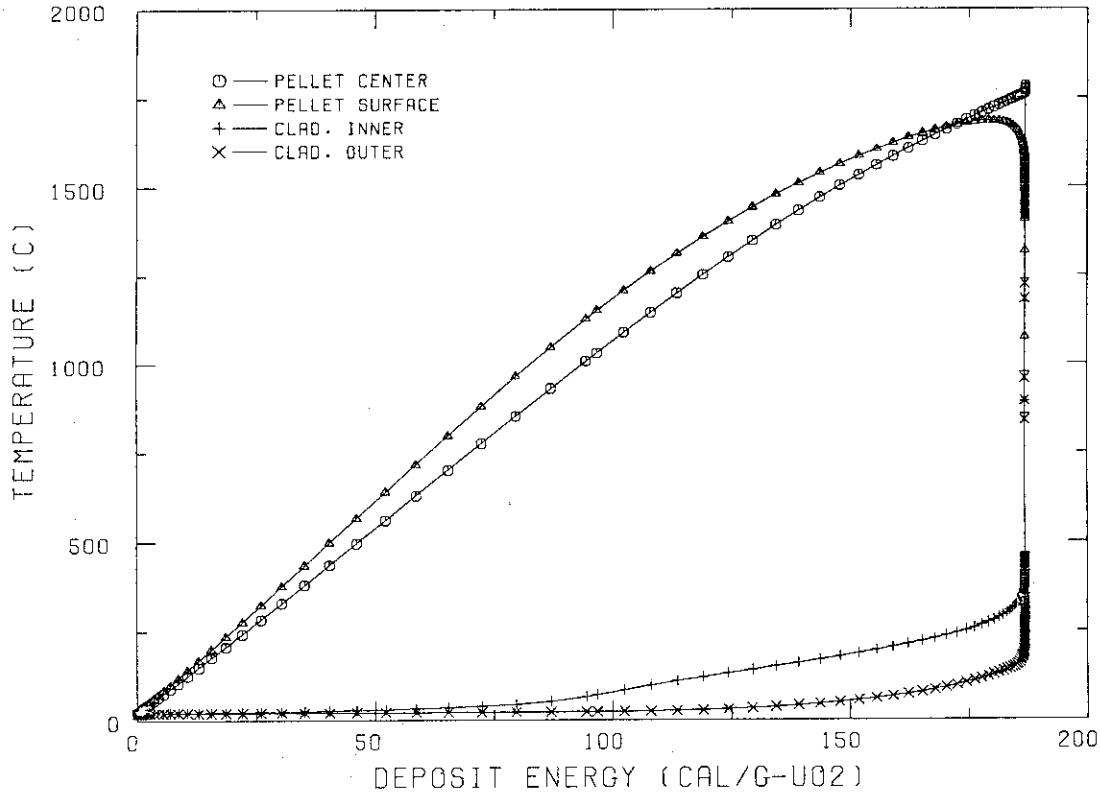

Fig. 5 Calculated pellet and cladding temperatures at the axial peak power location during the SPERT/CDC test RIA (Test No. 685).

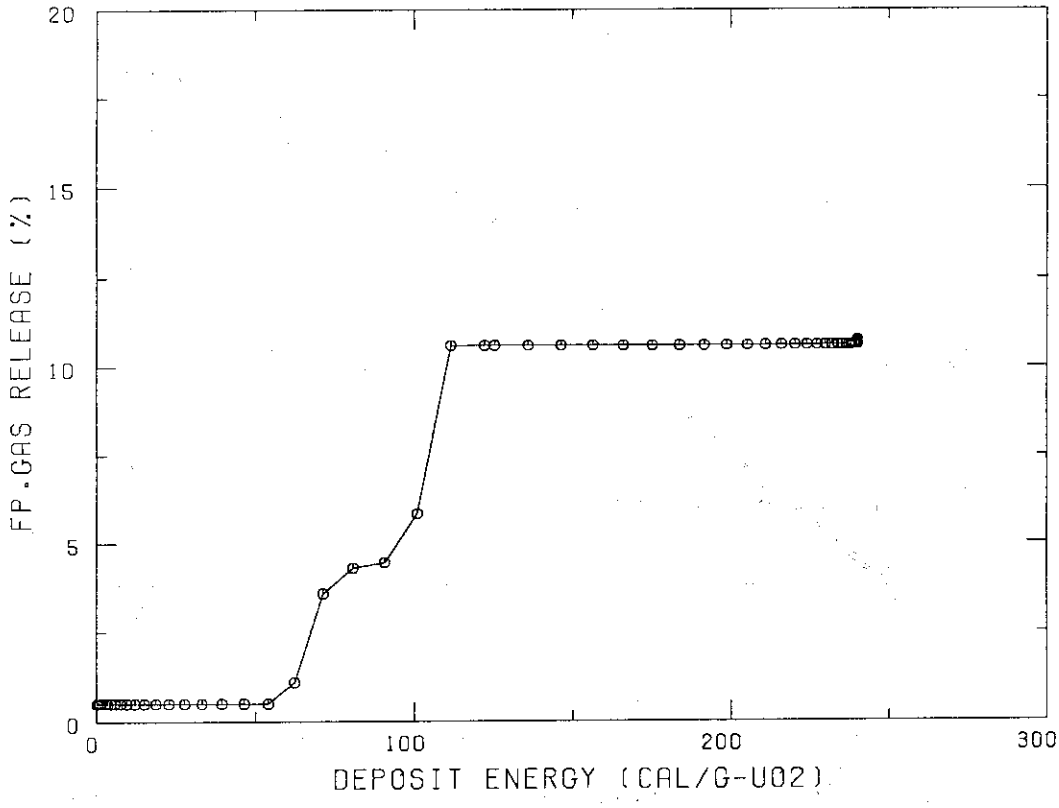

Fig. 6 Calculated fission gas release at the axial peak power location during the PBF test RIA 1-2 (Rod No. 802-2).

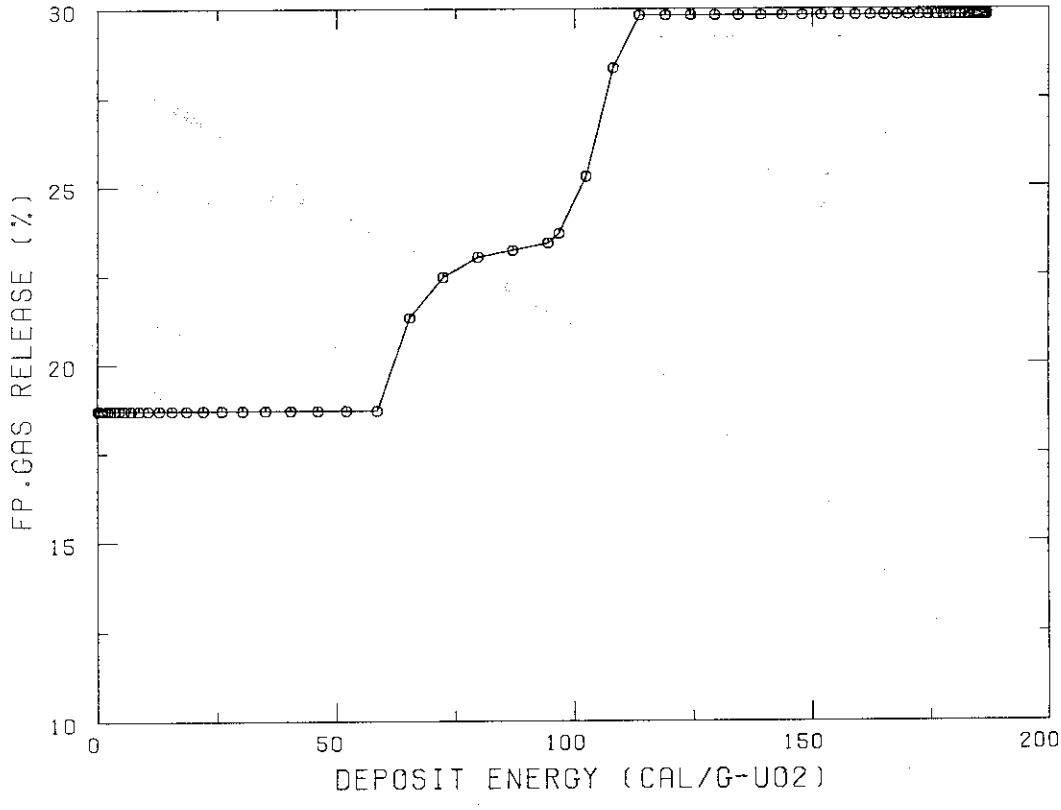

Fig. 7 Calculated fission gas release at the axial peak power location during the SPERT/CDC test RIA (Test No. 685).

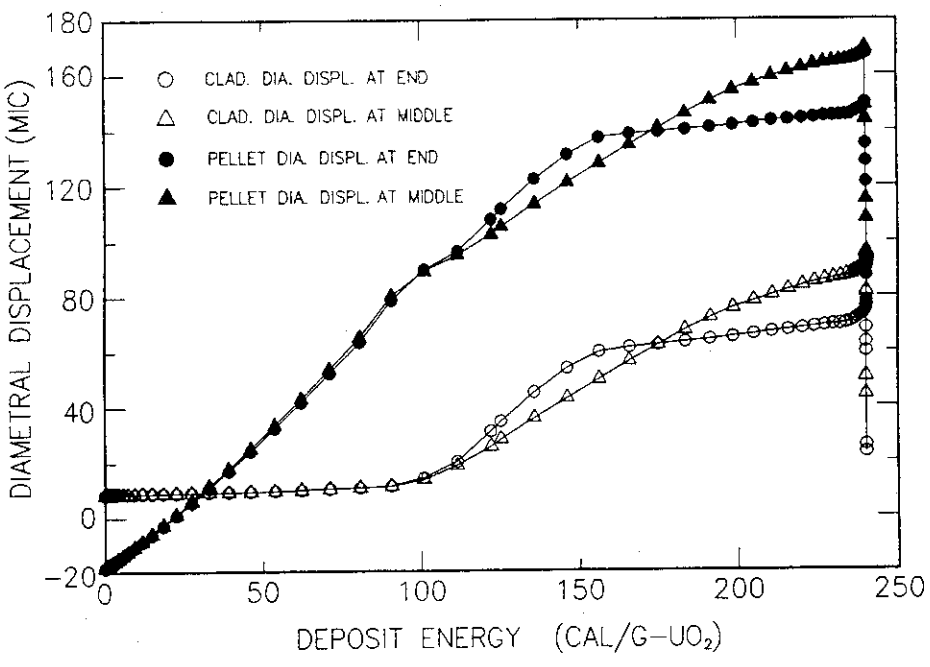

Fig. 8 Calculated cladding and pellet diametral displacements at the pellet end and middle positions at the axial peak power location during the PBF test RIA 1-2 (Rod No. 802-2).

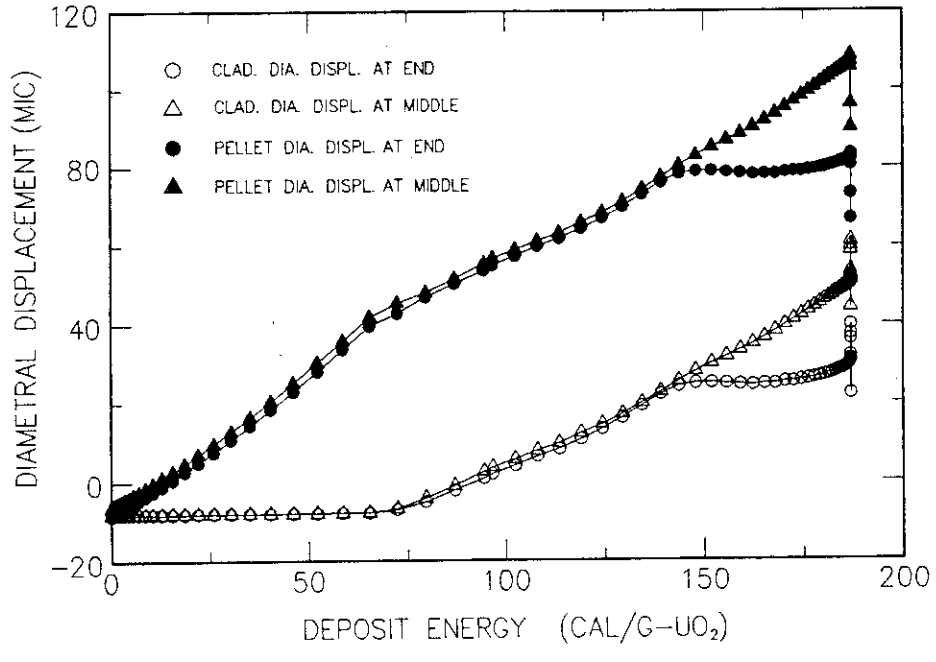

Fig. 9 Calculated cladding and pellet diametral displacements at the pellet end and middle positions at the axial peak power location during the SPERT/CDC test RIA (Test No. 685).

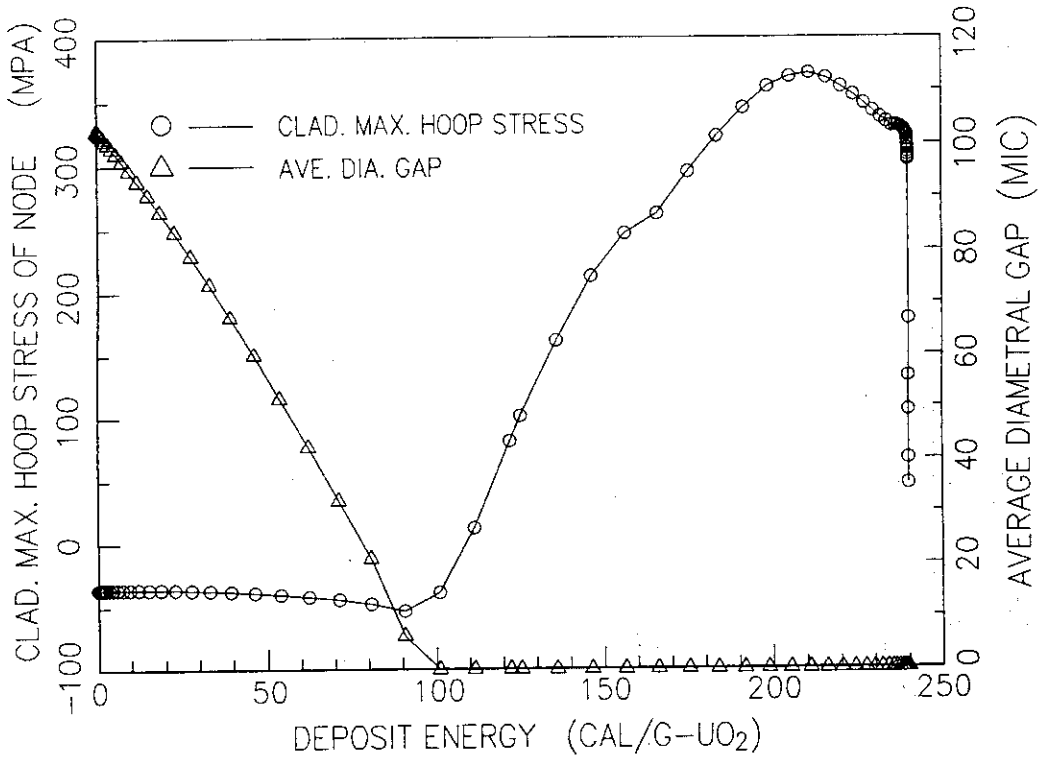

Fig. 10 Calculated cladding maximum hoop stress at each time step and average diametral gap at the axial peak power location during the PBF test RIA 1-2 (Rod No. 802-2).

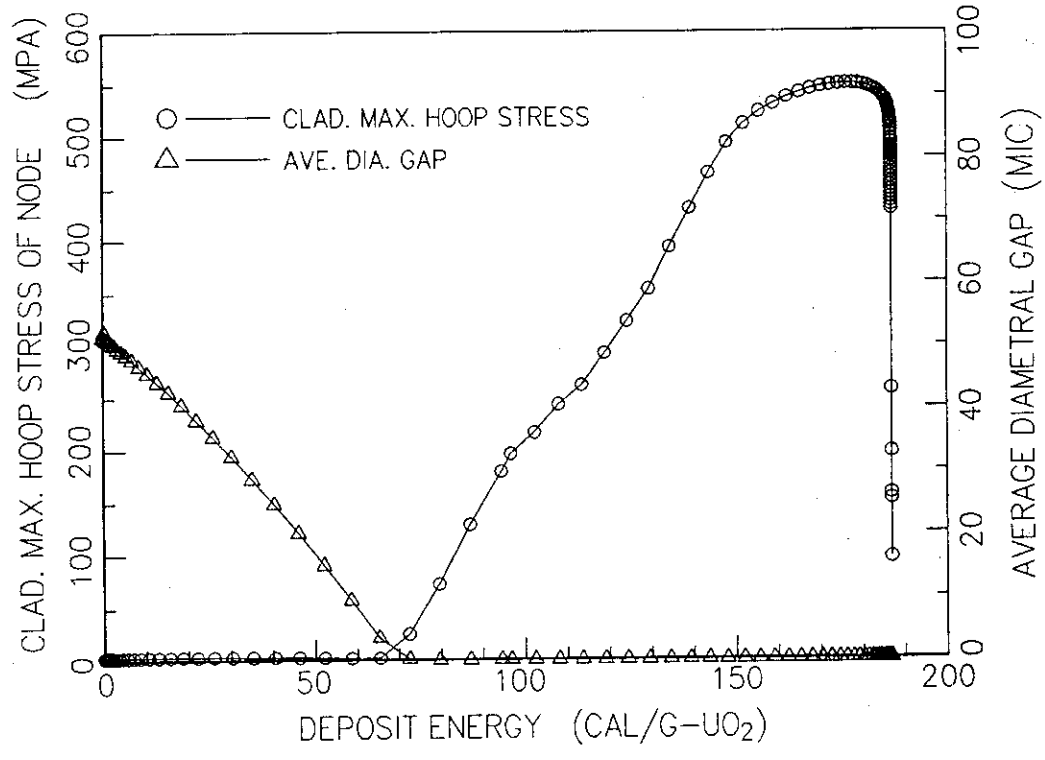

Fig. 11 Calculated cladding maximum hoop stress at each time step and average diametral gap at the axial peak power location during the SPERT/CDC test RIA (Test No. 685).

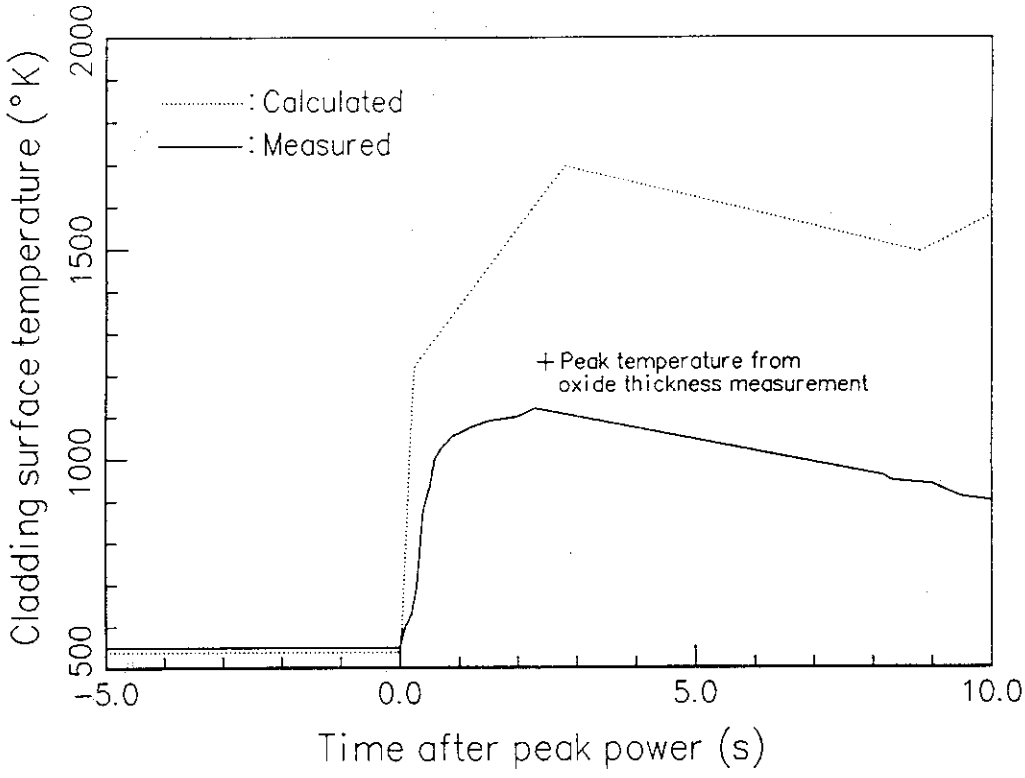

Fig. 12 Calculated and measured cladding surface temperatures at the 0.79 m BOF location for the PBF test RIA 1-2 (Rod No. 802-1).

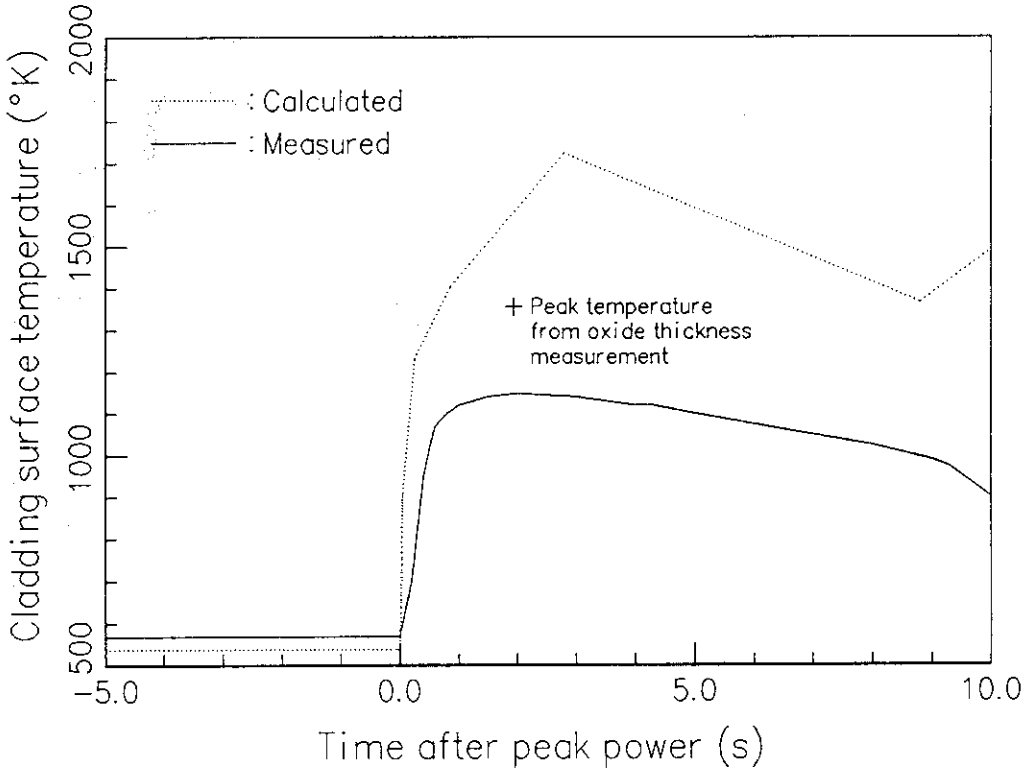

Fig. 13 Calculated and measured cladding surface temperatures at the 0.79 m BOF location for the PBF test RIA 1-2 (Rod No. 802-2).

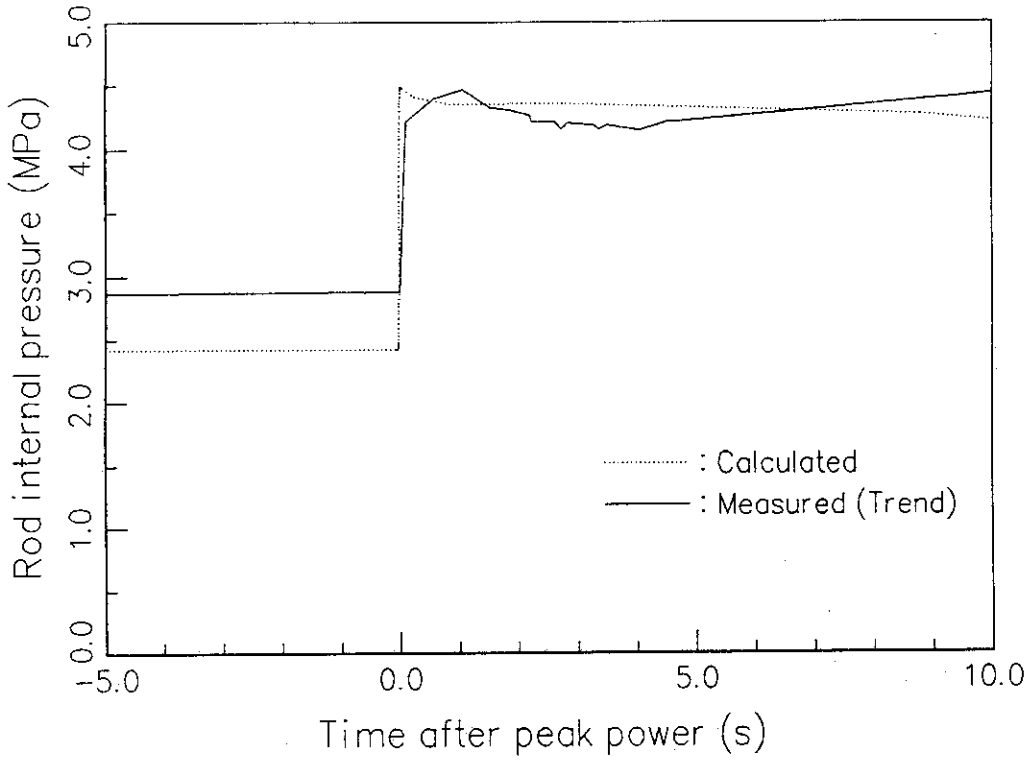

Fig. 14 Calculated and measured rod internal pressures for the PBF test RIA 1-2 (Rod No. 802-2).

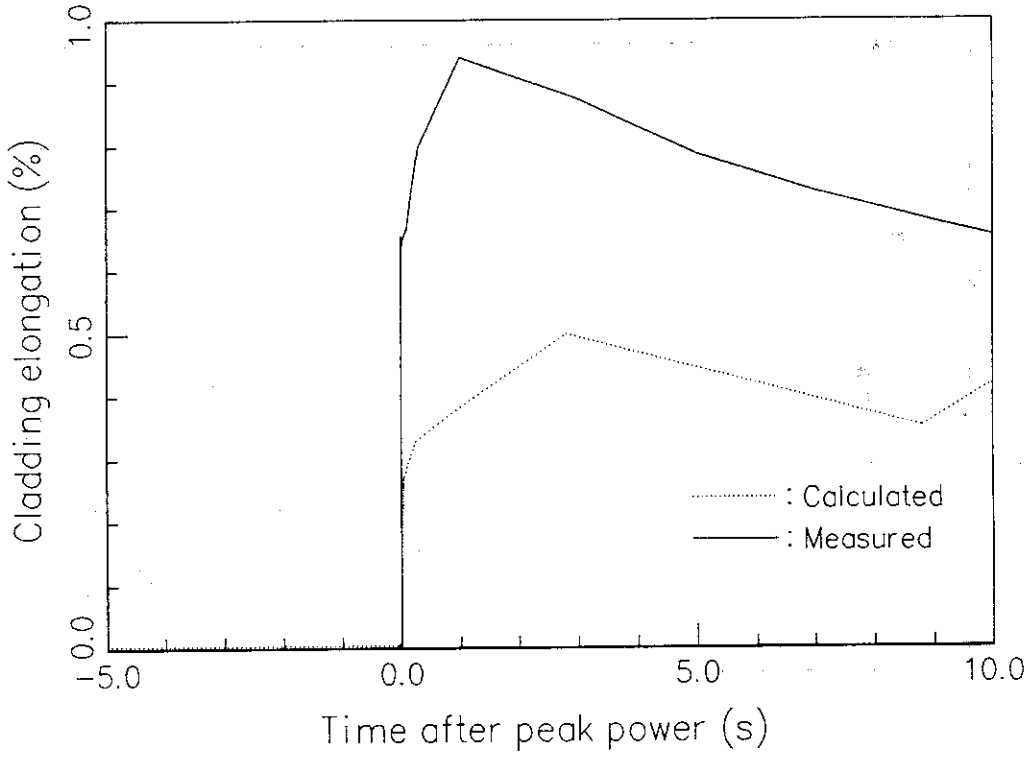

Fig. 15 Calculated and measured cladding elongations for the PBF test RIA 1-2 (Rod No. 802-2).

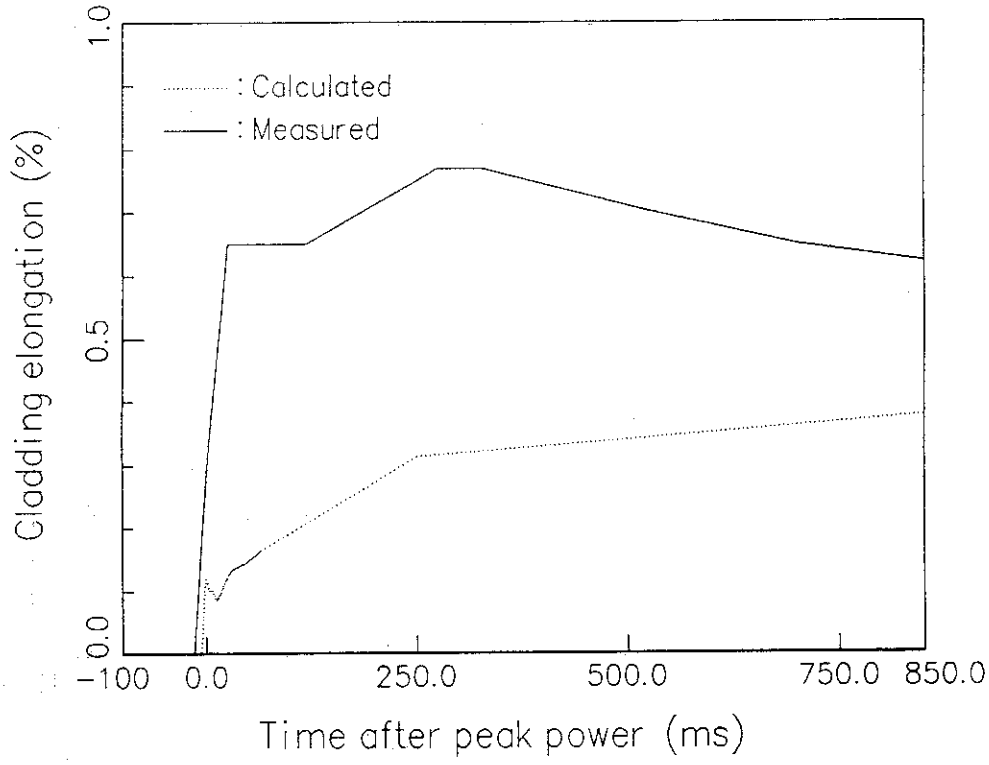

Fig. 16 Calculated and measured cladding elongations for the SPERT/CDC test RIA (Test No. 685).

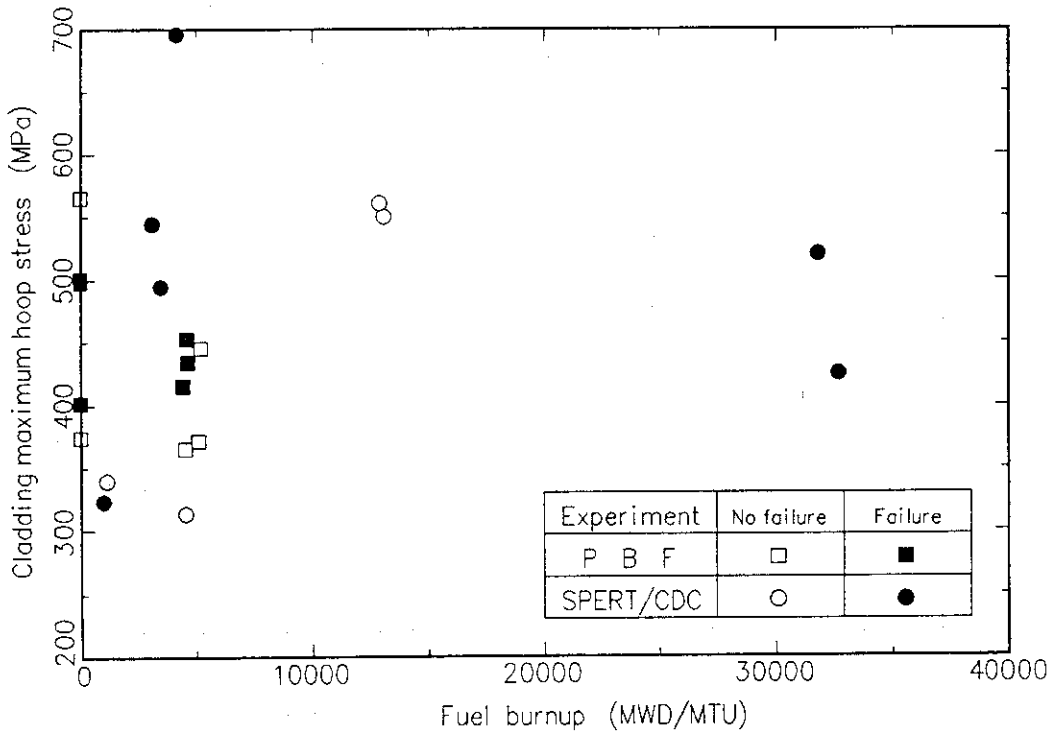

Fig. 17 Calculated cladding maximum hoop stress vs. Preirradiation burnup.

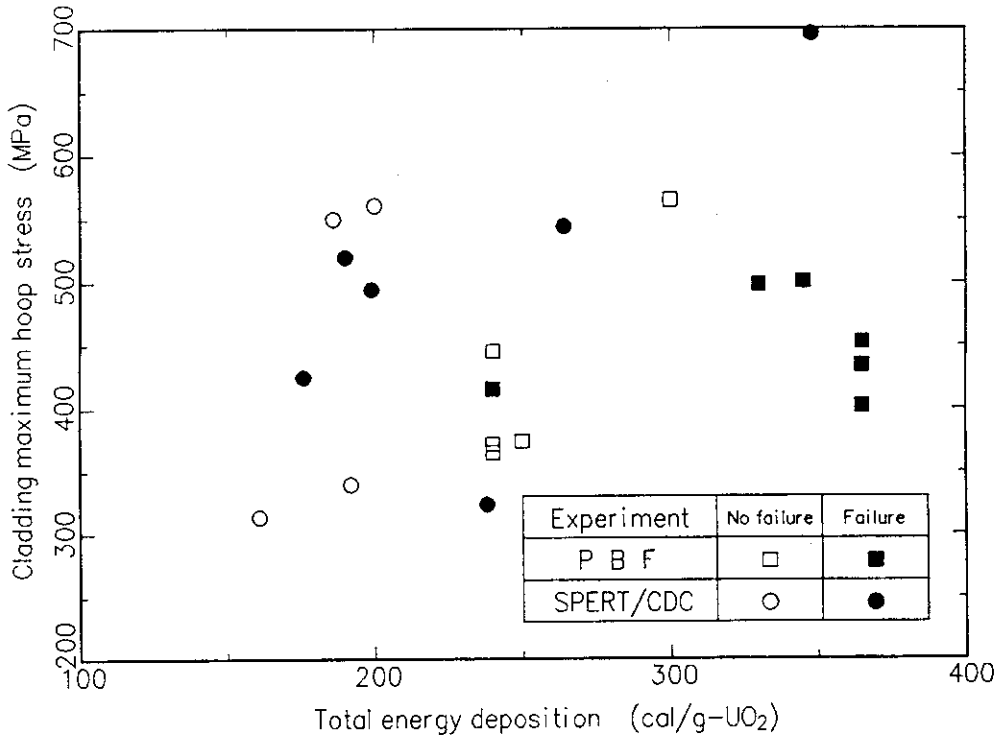

Fig. 18 Calculated cladding maximum hoop stress vs. Total energy deposition.